Molecular Docking, ADMET Prediction, and Quantum Computational on 2-Methoxy Benzoyl Hydrazone Compounds as Potential Antileishmanial Inhibitors

Ayoub Khaldan [1,*] 🆔, **Soukaina Bouamrane** [1], **Reda El-mernissi** [1], **Hamid Maghat** [1], **Abdelouahid Sbai** [1,*], **Mohammed Bouachrine** [1,2], **Tahar Lakhlifi** [1]

[1]   Molecular Chemistry and Natural Substances Laboratory, Faculty of Science, University Moulay Ismail, Meknes, Morocco; a.khaldan@edu.umi.ac.ma (A.K.); s.bouamrane@edu.umi.ac.ma (S.B); re.elmernissi@edu.umi.ac.ma (R.E); h.maghat@umi.ac.ma (H.M); sbai.abdelouahid@hotmail.com (A.S); bouachrine@gmail.com (M.B.); tahar.lakhlifi@yahoo.fr (T.L.);

[2]   EST Khenifra, Sultan Moulay Sliman University, Benimellal, Morocco; bouachrine@gmail.com (M.B.);

*   Correspondences: sbai.abdelouahid@hotmail.com (A.S); a.khaldan@edu.umi.ac.ma (A.K.);

Abstract: Leishmaniasis is a neglected disease that affects about one million people a year worldwide and is present in over 90 countries. This illness is a serious public health issue since it can result in mutilation, incapacity, and even death. The drugs currently used for treatment are highly toxic, ineffective, expensive, and may cause antiparasitic resistance. A series of twenty-five 2-methoxy benzoyl hydrazone derivatives have recently been identified as promising antileishmanial inhibitors and was addressed using a molecular docking approach. All docked compounds interacted well within the active pocket of the receptor. Compounds **M12**, **M15**, **M16**, and **M20** show a good binding energy value of -9.40, -8.90, -9.00, and -9.20 Kcal/mol, respectively, compared to pentamidine (-8.20 Kcal/mol), used as reference drug. These molecules also present many types and numbers of interactions with the studied receptor. The studied molecules were evaluated for their pharmacokinetic properties using ADMET prediction. They showed good bioavailability, particularly the molecules M12, M15, and M16 which were found to be non-toxic. Quantum calculations using the DFT approach were performed on the four selected compounds to determine the most electrophilic and nucleophilic of them. These findings would be very helpful in the search for new antileishmanial inhibitors.

Keywords: molecular docking; ADMET; DFT; antileishmanial.

1. Introduction

Leishmaniasis is a neglected tropical illness found in more than 90 countries in Africa, Asia, and the Americas [1]. According to the WHO, 350 million people globally reside in risk zones, and each year there are about two million new leishmaniasis cases [2]. The parasite is spread from invertebrate hosts to mammalian hosts by female sandflies. Visceral leishmaniasis (VL) and cutaneous leishmaniasis (CL) are the two main clinical forms of leishmaniasis. The former is characterized by cutaneous and/or mucosal lesions, while the latter is produced when the parasites have a tropism for internal organs, such as the liver and spleen. VL is the most severe form of illness and is fatal if untreated [3]. *Leishmania infantum* in Central Asia,

Mediterranean Basin, Central America, and South America, and *Leishmania donovani* in Asia and Africa are the two species that cause VL, respectively [4,5].

Pentavalent antimonials, including miltefosine, sodium stibogluconate, amphotericin B, paromomycin, and pentamidine, are the basis of modern leishmaniasis chemotherapy. However, many of these medications exhibit severe toxicity, result in clinical resistance, and promote co-infections such as leishmaniasis-AIDS [6,7]. Additionally, these medications are very expensive and necessitate ongoing care [8]. Therefore, finding newer compounds to combat Leishmania species is urgently needed [9].

Heterocyclic hydrazones compounds are very interesting scaffolds in organic chemistry. They have been documented as having numerous biological activities such as antifungal, anti-HIV, antibacterial [10,11], and antimicrobial [12]. Due to their strong affinity for chelation, suited for solid metal complexes, Schiff bases serve as models for biologically known species [13]. Schiff bases have various biological impacts, notably antifungal, anticancer, antibacterial, anti-inflammatory, and antioxidant properties [14–16].

Computational chemistry plays a very important role in drug design. It reduces time, effort, and cost and gives fast and accurate results before moving to experimentation [17–19]. Therefore, computational chemistry can be considered an essential and primary step in molecule synthesis [20]. Molecular docking is one of the main techniques in computational chemistry. It is widely adopted in the bio-organic chemistry field due to its fast and efficient use. It provides explanations of the patterns of interactions between the receptor and the ligand and thus allows guessing the stability of the compounds in the receptor's active site [21–23].

Pharmacokinetics, including ADMET (absorption, distribution, metabolism, excretion, and toxicity) prediction and drug-likeness rules, have taken the lead in further research to characterize bioavailability and examine the toxicity of compounds [24–27]. It provides insights into a molecule before it is synthesized.

The current study aims to identify lead candidate compounds that could be adopted as future leishmaniasis inhibitors using a molecular docking approach. ADMET properties were predicted for the studied molecules to identify compounds with favorable pharmacokinetic properties. Finally, quantum calculations were performed to determine the most electrophilic and nucleophilic 2-methoxy benzoyl hydrazone compounds.

2. Materials and Methods

2.1. Dataset.

In this research, twenty-five 2-methoxy benzoyl hydrazone compounds were selected from the literature [28]. These compounds were synthesized by Taha et al. using simple techniques and substrates and evaluated for their antileishmanial activity (IC_{50}) [28]. The investigated molecules were considered for molecular docking and ADMET study. The antileishmanial activity (IC_{50}) values were transformed into an equivalent pIC_{50} values using the following expression: $pIC_{50} = -log_{10}(IC_{50})$.
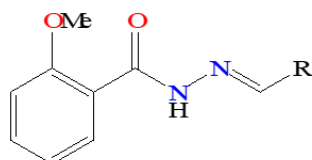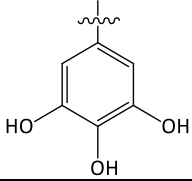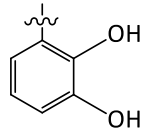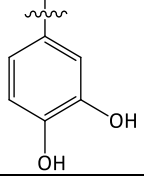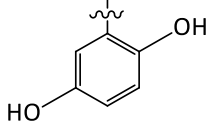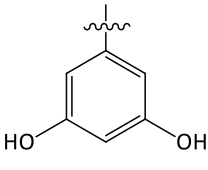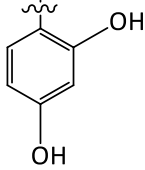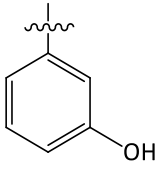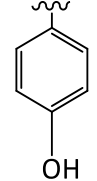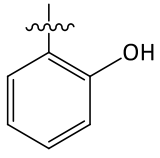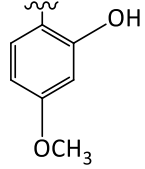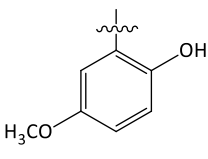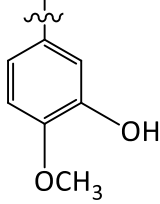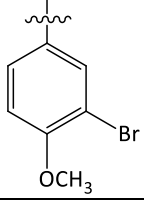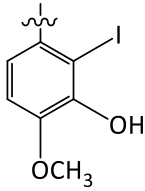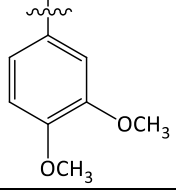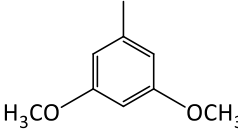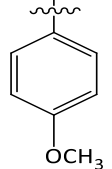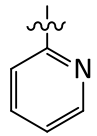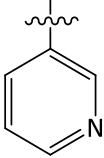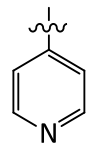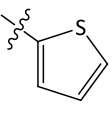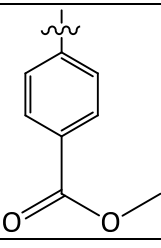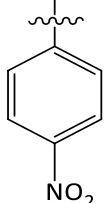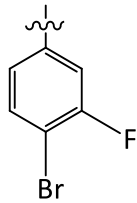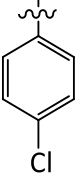

Figure 1. 2-methoxy benzoyl hydrazone compounds chemical structure.

The chemical structure and antileishmanial activity of the 25 molecules studied are presented in Figure 1 and Table 1.

Table 1. Chemical structures of the investigated molecules and their pIC_{50} values.

Comp N°	R	pIC_{50}	Comp N°	R	pIC_{50}
1		4.426	14		4.167
2		5.483	15		4.458
3		4.549	16		4.053
4		4.479	17		4.241
5		4.451	18		4.870
6		3.996	19		4.340
7		5.117	20		4.198
8		4.880	21		4.275
9		4.397	22		4.222

Comp N°	R	pIC$_{50}$	Comp N°	R	pIC$_{50}$
10		5.710	**23**		4.120
11		5.604	**24**		4.805
12		4.501	**25**		4.111
13		4.164			

2.2. Ligands drawing and optimization.

The 25 studied molecules were sketched using SYBYL-X 2.0 software. Then, they were optimized using Gaussian G09 software [29] and using density function theory (DFT) with a B3LYP/6-311++G (d,p) basis set to achieve the equilibrium geometry.

2.3. Molecular docking study.

The molecular docking method is performed to obtain a deeper understanding of the binding modes and to predict potential interactions between 2-methoxy benzoyl hydrazone compounds and the receptor [30]. In this paper, molecular docking simulation was executed by using Autodock Vina [31] and Autodock tools 1.5.6 [32] programs. The crystal structure of the selected receptor was taken from RCSB (PDB ID: 2JK6) [33,34] with a resolution of 2.95 Å. Then, it was prepared by deleting all the water molecules and adding the polar hydrogen atoms using Discovery Studio 2016 program [35]. The box grid was constructed in the following directions x = 30, y = 30, z = 30 inside the pocket of the target receptor with a spacing of 1 Å between grid points. The coordinates of the center of the network are defined as x= 29.416, y= 50.327, and z= -2.014. Using the Autodock 1.5.6 tool, an extended PDB format named PDBQT is employed for coordinate files carrying atomic partial charges and atom types [36] for ligand and receptor preparations. The flexible and non-bonded rotation of selected ligands is defined using torsion angles [36]. Afterward, the 2-methoxy benzoyl hydrazine ligands were docked into the active pocket of the studied receptor. The generated outcomes were analyzed using the Discovery Studio 2016 [35] software.

2.4. In silico ADMET analysis.

The synthesis/prediction of a molecule is viewed as an essential step in searching for new agents for treating certain diseases. Indeed, for a molecule to be certified and adopted as a future drug, it must pass through four steps: absorption, distribution, metabolism, excretion, and toxicity (ADMET). The 25 studied molecules were evaluated for their ADMET properties using pkCSM [37] and SwissADME [38] online servers for this great goal.

2.5. Global properties of the 2-methoxy benzoyl hydrazone molecules using the DFT approach.

Using the DFT approach, the global reactivity indices such as chemical potential (μ), chemical softness (S), chemical hardness (η), global nucleophilicity, and global electrophilicity (ω) were calculated for the 2-methoxy benzoyl hydrazone molecules to identify the most electrophilic and nucleophilic inhibitors. In fact, the chemical potential (μ) was computed based on the frontier molecular orbital HOMO and LUMO by the formula as follows $\mu = (E_{HOMO} + E_{LUMO})/2$. The chemical hardness (η) and chemical softness (S) were determined by the following equations $\eta = E_{LUMO} - E_{HOMO}$ and $S = 1/\eta$ [39], respectively. The global electrophilicity (ω) [40] and global nucleophilicity (N) [41] were derived from the following expression $\omega = \mu^2/2\eta$ and $N = E_{HOMO}(Nu) - E_{HOMO}(TCE)$, respectively, tetracyanoethylene (TCE) was selected as a calculation reference because it has a lower HOMO energy value [41,42].

3. Results and Discussion

3.1. Molecular docking result.

3.1.1. Binding energy and inhibition constant of the targeted molecules

The 25 selected molecules were docked into the active pocket of the 2JK6 receptor. The results of binding energy and inhibition constant are presented in Table 2. Compounds **M12**, **M15**, **M16**, and **M20** show good binding energy values compared to dataset molecules and reference drug (Pentamidine), indicating that these compounds have good stability and interact well with the receptor. Therefore, in the part of molecular docking interactions result, we will focus only on these molecules. Furthermore, from the binding energy (ΔG), the inhibition constant (Ki) was derived using the following expression: Ki = exp(ΔG/RT), where R is the universal gas constant (1.985×10^{-3} kcal mol^{-1} K^{-1}) and T is the temperature (298.15 K). In fact, the lower the Ki value, the greater the drug's efficacy [43]. The result in Table 2 clearly indicates that the four molecules mentioned above have smaller Ki, especially compound **M12**. These molecules are, therefore, more effective than pentamidine.

Table 2. Binding energy and inhibition constant (Ki) of the **25** studied molecules.

Compound	Binding energy (Kcal/mol)	Inhibition constant Ki (μM)	Compound	Binding energy (Kcal/mol)	Inhibition constant Ki (μM)
M1	-8.40	0.685	**M14**	-8.20	0.960
M2	-8.50	0.578	**M15**	**-8.90**	**0.294**
M3	-8.30	0.811	**M16**	**-9.00**	**0.248**
M4	-8.30	0.811	**M17**	-8.60	0.488
M5	-8.60	0.488	**M18**	-8.70	0.412
M6	-8.70	0.412	**M19**	-8.70	0.412
M7	-8.60	0.488	**M20**	**-9.20**	**0.177**
M8	-8.80	0.348	**M21**	-8.80	0.348

Compound	Binding energy (Kcal/mol)	Inhibition constant Ki (μM)	Compound	Binding energy (Kcal/mol)	Inhibition constant Ki (μM)
M9	-8.40	0.685	**M22**	-8.60	0.488
M10	-8.20	0.960	**M23**	-8.30	0.811
M11	-7.70	2.236	**M24**	-8.70	0.412
M12	**-9.40**	**0.126**	**M25**	-8.80	0.348
M13	-8.80	0.348	Pentamidine	-8.20	0.960

3.1.2. Molecular docking interaction.

The compound **M12** was docked into the active site of the 2JK6 receptor, and its findings are shown in Figure 2. The nitrogen oxide (-NO2) group of the compound **M12** affords 3 conventional hydrogen bonding interactions with Gly15, Ser14, and Asp327 residues at distances of 2.82, 3.16, and 3.32 Å, respectively. The phenyl ring bound to the nitrogen oxide provides a pi-alkyl interaction with the Ala338 residue at a distance of 5.09 Å and a pi-anion interaction with the Asp327 residue at a distance of 3.72 Å. The 2-methoxy benzoyl group forms three types of interactions with the concerned receptor: a pi-alkyl with residues Cys57, Ile199, and Lys60 at distances of 5.32, 4.93, and 4.82 Å, respectively, a carbon-hydrogen bond with residues Ser178 and Val55 at distances of 3.75 and 3.40 Å, respectively, and a pi-donor hydrogen bond with residue Tyr198 (3.72 Å). The ketone party exhibits a conventional hydrogen bonding interaction with Tyr198 (3.22Å) residue. Therefore, the existing interactions give the molecule **M12** good stability in the receptor's active pocket.

The molecular docking result of compound **M15** shows three conventional hydrogen bonding interactions with Ser14 (3.21Å), Tyr198 (2.88Å), and Arg287 (3.34Å) residues, two pi-donor hydrogen bonding interactions with Thr335 (3. 98Å) and Serr14 (3.80Å) residues, a pi-sigma interaction with Ile199 (3.67Å) residue, a pi-anion interaction with Asp327 (4.22Å) residue, and a pi-alkyl interaction with Ala338 (4.89Å) residue (Figure 3). In the case of compound **M16**, there are numerous types and numbers of interactions (Figure 4). Three conventional hydrogen bond interactions with Thr335 (2.95Å), Gly15 (3.32Å), and Arg287 (3.13Å) residues, three pi-donor hydrogen bond interactions with residues Ser14 (3.64Å), Thr335 (4.12Å) and Tyr198 (4.14Å), two pi-alkyl interactions with Ala338 (4.85Å) and Lys60 (5.44Å) residues, a pi-anion interaction with Ile199 (3.93Å) residue at a distance f, a pi-anion interaction with Asp327 (4.47Å) residue, and an- amide-pi stacked interaction with Gly56 (4.38Å) residue. Finally, the compound **M20** affords favorable interactions like conventional hydrogen bonds with the following residues Asp237 (2.05Å), Cys52 (3.07Å), Thr51 (3.08Å) and Lys60 (3.37Å), pi-donor hydrogen bond with Tyr198 (3.41Å) residue, amide-pi stacked with Gly56 (4.50Å) residue, pi-pi T-shaped with Gly56 (5.64Å) residue, pi-anion with Asp327 (4.79Å) residue, alkyl with Cys57 (4.37Å), and pi-alkyl with Cys57 (4.90Å) residue (Figure 5). The important number of hydrogen bonding interactions gives compound **M20** great pharmacological importance as hydrogen bonds heavily affect the pharmacological action of ligands. On the other hand, to give reliability to this study and to confirm the predictive power of the docking results, pentamidine, which is used clinically as a reference drug, was also docked into the active pocket of the studied receptor, and its result is presented in Figure 6. In fact, pentamidine affords three conventional hydrogen bond interactions with Met333 (2.36Å), Thr335 (2.15 Å), and Gly127 (2.29Å) residues, two pi-sigma interactions with Val36 (3.82 Å) and Thr160 (3.80Å) residue and others interactions with different residues and distances. In conclusion, the selected compounds M12, M15, M16, and M20 have good binding energy values, lower inhibition constant, and many types and interactions than pentamidine.
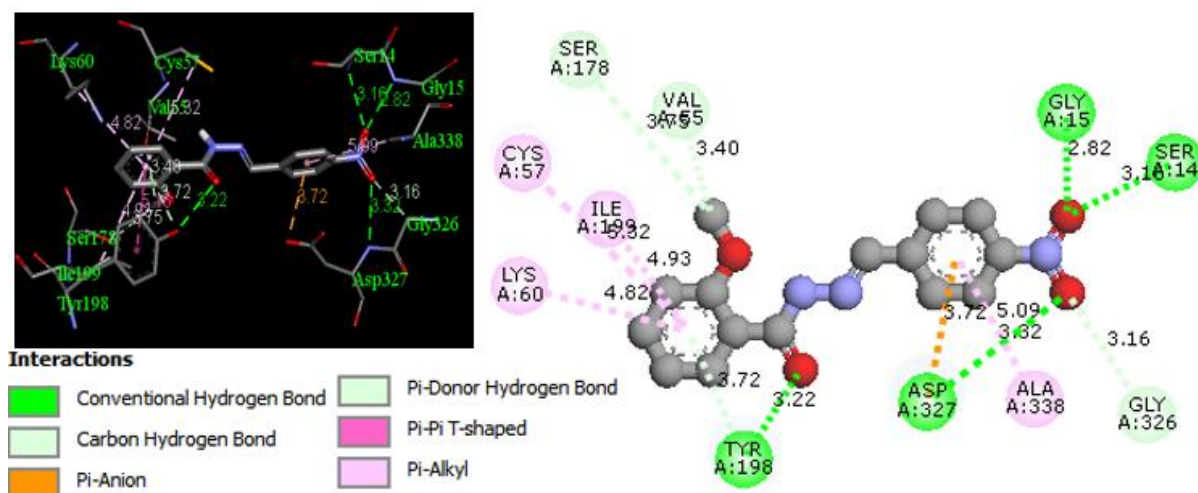
Figure 2. Visualizations of 3D (right) and 2D (left) interactions for the molecule **M12** docked into studied receptor 2JK6.
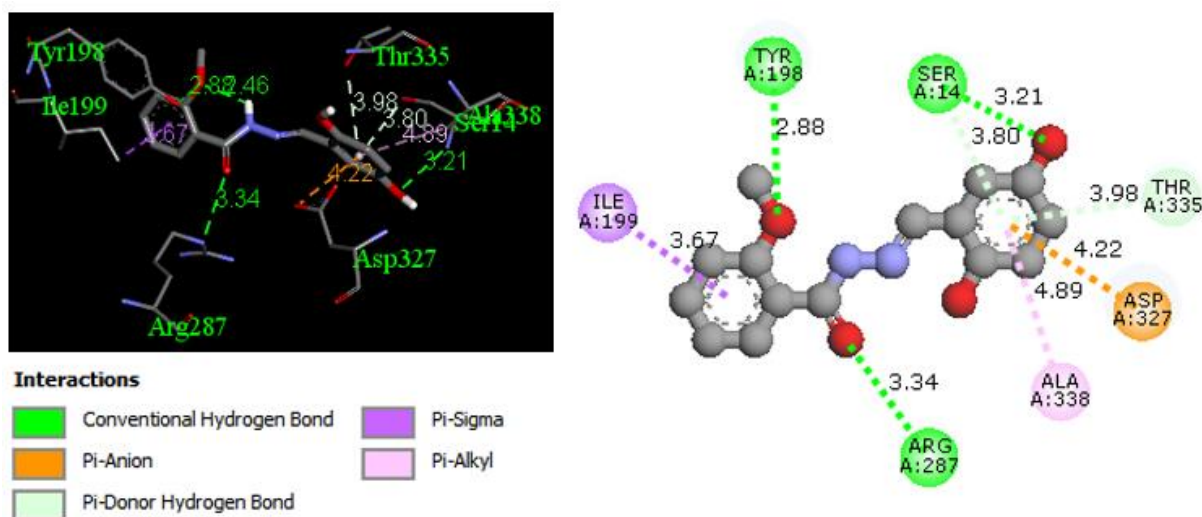
Figure 3. Visualizations of 3D (right) and 2D (left) interactions for the molecule **M15** docked into studied receptor 2JK6.
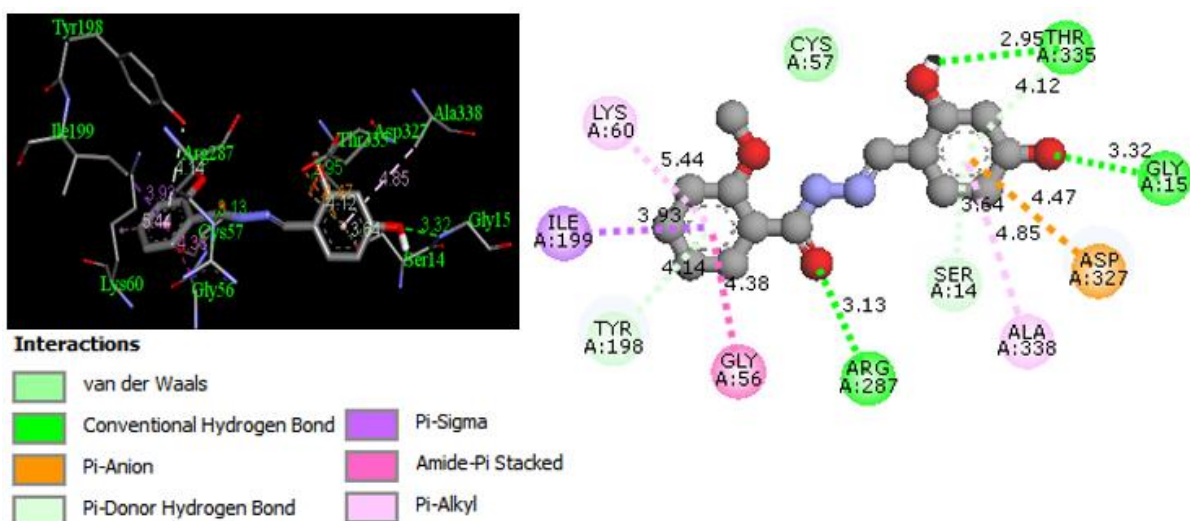
Figure 4. Visualizations of 3D (right) and 2D (left) interactions for the molecule **M16** docked into studied receptor 2JK6.
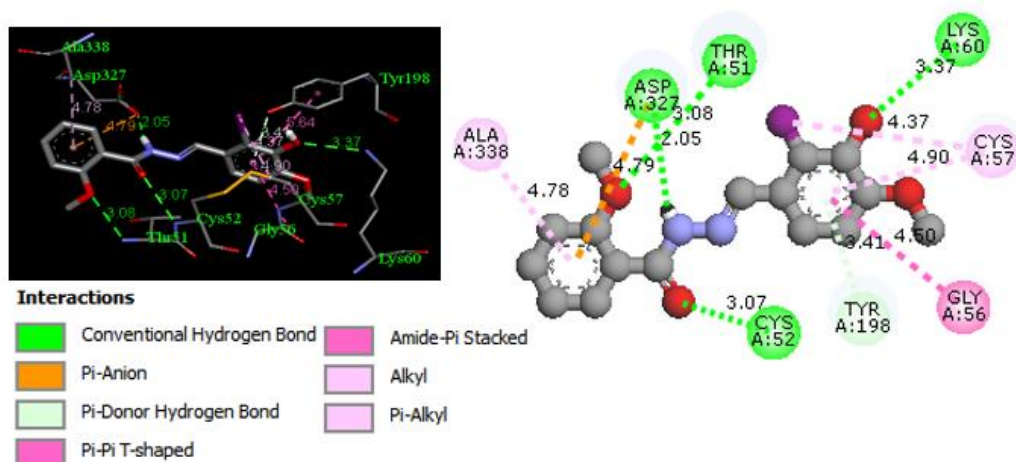
Figure 5. Visualizations of 3D (right) and 2D (left) interactions for the molecule **M20** docked into studied receptor 2JK6.
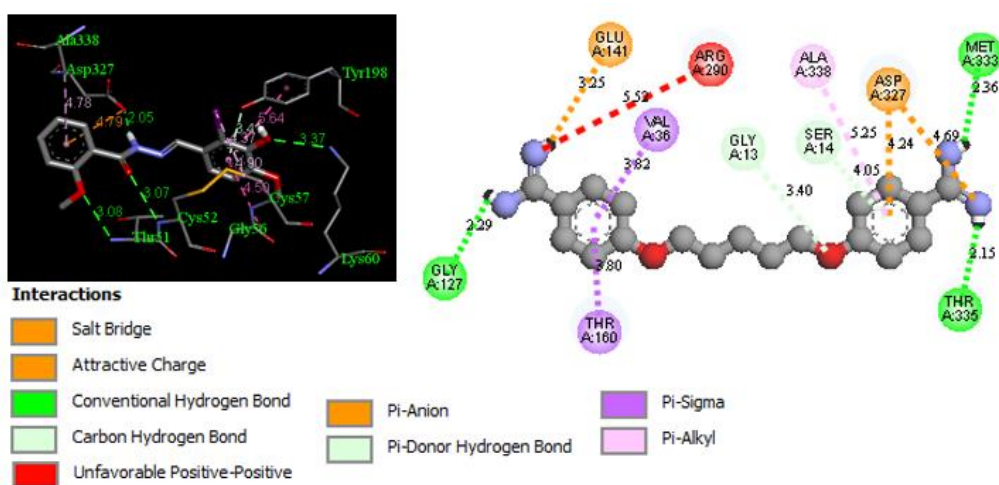
Figure 6. Visualizations of 3D (right) and 2D (left) interactions for the pentamidine drug docked into studied receptor 2JK6.

3.1.3. Molecular docking validation.

The reliability of the molecular docking technique was validated by re-docking. The overlaid view of the original ligand (red color) and the re-docked conformation (magenta color) is displayed in Figure 6.
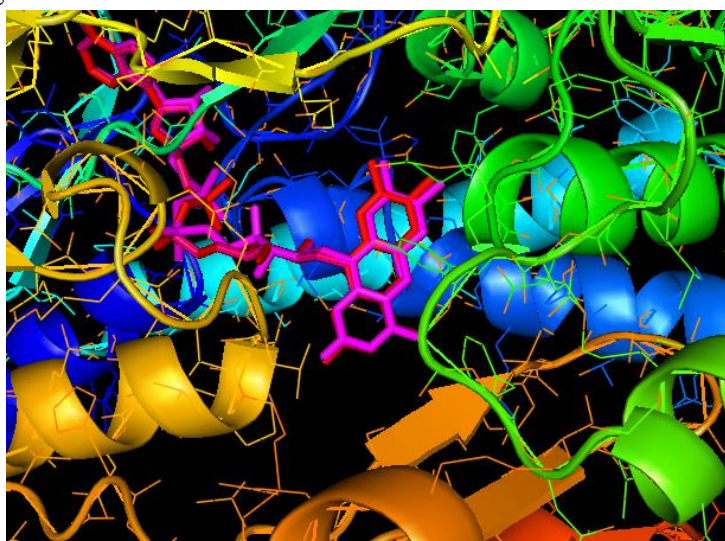
Figure 7. Re-docking pose of the co-crystalized ligand Å (Red = Original, Magenta = Docked).

The result of re-docking indicated a good overlay between the original and re-docked conformation. The docked ligand's root means square distance (RMSD) is 0.541 Å which was inside the reliable range of 2 Å [44]. Therefore, the good overlap between the two ligands as well as the lower value of RMSD (less than 2 Å), confirmed the ability of Autodock Vina software to carry out molecular docking protocols confidently.

3.2. Pharmacokinetic properties and drug-likeness results of the 25 studied molecules.

The pkCSM [37] and SwissADME [38] online programs were applied to predict the pharmacokinetic properties of the twenty-five 2-methoxy benzoyl hydrazone compounds, and the obtained results are shown in Table 3. A given molecule with logP < 5, molecular weight < 500, hydrogen bond acceptor number < 10, and hydrogen bond donor number < 5 is considered to have the best oral absorption and permeation [45]. The result of Table 3 indicates that all studied molecules have good absorption and permeation. On the other hand, a compound with a total polar surface area (TPSA) below 140 Å^2 and a number of rotatable bonds (nrotb) not over 10 present excellent bioavailability. It becomes more pliable to interact with a specific binding pocket successfully. All investigated molecules have good bioavailability and are more flexible. Good solubility of a compound is reflected by a logS value not greater than 6. Thus, all selected compounds have good solubility (Table 3). The Csp3 fraction is defined as the ratio of sp3 hybridized carbons to the total number of carbons in the molecule; its value would have to be at least 0.25. From the results of Table 3, all molecules have good saturation. Moreover, molecule with $250 \leq$ MW (g/mol) ≤ 350, logP $\leq$ 3.5 and nrotb ≤ 7 considered as lead-likeness [46]. With the exception of compounds **M7**, **M9**, **M20**, and **M25**, all studied molecules are lead-likeness. The result in Table 4 shows that all molecules are in full compliance with the most significant drug-likeness rules, Lipinski, Ghose, Veber, Egan, and Muegge, and they exhibited a score of 55%; demonstrating their better bioavailability [46].

Table 3. Molecular properties descriptors and lead-likeness of the 25 2methoxy benzoyl hydrazone compounds.

| N°	Property									
	Formula	MW	HBD	HBA	nrotb	LogP	TPSA	LogS	CSp^3	Lead-likeness
M1	$C_{15}H_{14}N_2O_5$	302.28	4	6	4	4.00	111.38	-2.88	0.07	Yes
M2	$C_{15}H_{14}N_2O_4$	286.28	3	5	5	1.87	91.15	-3.02	0.07	Yes
M3	$C_{15}H_{14}N_2O_4$	286.28	3	5	5	1.87	91.15	-2.92	0.07	Yes
M4	$C_{15}H_{14}N_2O_3$	270.28	2	4	4	2.16	70.92	-3.17	0.07	Yes
M5	$C_{15}H_{14}N_2O_3$	270.28	2	4	4	2.16	70.92	-3.73	0.07	Yes
M6	$C_{16}H_{16}N_2O_4$	300.31	2	5	5	2.17	80.15	-3.79	0.12	Yes
M7	$C_{16}H_{15}BrN_2O_3$	363.21	1	4	5	3.23	59.92	-4.29	0.12	No
M8	$C_{17}H_{18}N_2O_4$	314.34	1	5	6	2.47	69.15	-3.28	0.18	Yes
M9	$C_{16}H_{16}N_2O_3$	284.31	1	4	5	2.46	59.92	-3.94	0.12	No
M10	$C_{14}H_{13}N_3O_2$	255.27	1	4	4	1.85	63.58	-2.65	0.07	Yes
M11	$C_{13}H_{12}N_2O_2S$	260.31	1	4	4	2.52	78.63	-3.35	0.08	Yes
M12	$C_{15}H_{13}N_3O_4$	299.28	1	5	5	2.36	96.51	-3.25	0.07	Yes
M13	$C_{15}H_{13}ClN_2O_2$	288.73	1	3	4	3.11	50.69	-3.80	0.07	Yes
M14	$C_{15}H_{14}N_2O_4$	286.28	3	5	4	1.87	91.15	-3.59	0.07	Yes
M15	$C_{15}H_{14}N_2O_4$	286.28	3	5	4	1.87	91.15	-3.59	0.07	Yes
M16	$C_{15}H_{14}N_2O_4$	286.28	3	5	4	1.87	91.15	-3.59	0.07	Yes
M17	$C_{15}H_{14}N_2O_3$	270.28	2	4	4	2.16	70.92	-3.73	0.07	Yes
M18	$C_{16}H_{16}N_2O_4$	300.31	2	5	5	2.17	80.15	-3.79	0.12	Yes
M19	$C_{16}H_{16}N_2O_4$	300.31	2	5	5	2.17	80.15	-3.23	0.12	Yes
M20	$C_{16}H_{15}IN_2O_4$	426.21	2	5	5	2.77	80.15	-4.41	0.12	No
M21	$C_{17}H_{18}N_2O_4$	314.34	1	5	6	2.47	69.15	-3.33	0.18	Yes

N°	Property									
	Formula	MW	HBD	HBA	nrotb	LogP	TPSA	LogS	CSp^3	Lead-likeness
M22	$C_{14}H_{13}N_3O_2$	255.27	1	4	4	1.85	63.58	-2.86	0.07	Yes
M23	$C_{14}H_{13}N_3O_2$	255.27	1	4	4	1.85	63.58	-2.54	0.07	Yes
M24	$C_{17}H_{16}N_2O_4$	312.32	1	5	5	2.24	76.99	-3.56	0.12	Yes
M25	$C_{15}H_{12}BrFN_2O_2$	351.17	1	3	4	3.36	50.69	-4.37	0.07	No
Abbreviations	molecular weight (MW), number of hydrogen bonds donors (**HBD**), number of hydrogen bonds acceptors (**HBA**), number of rotatable bonds (**nrotb**), the logarithm of partition coefficient of compound between n-octanol and water (**Log**), Topological Polar Surface Area (**TPSA**), log S (calculated with the ESOL model.									

Table 4. Drug-likeness and bioavailability of the 25 studied molecules.

Compound	Lipinski	Ghose	Veber	Egan	Muegge	Bioavailability score
M1	Yes	Yes	Yes	Yes	Yes	0.55
M2	Yes	Yes	Yes	Yes	Yes	0.55
M3	Yes	Yes	Yes	Yes	Yes	0.55
M4	Yes	Yes	Yes	Yes	Yes	0.55
M5	Yes	Yes	Yes	Yes	Yes	0.55
M6	Yes	Yes	Yes	Yes	Yes	0.55
M7	Yes	Yes	Yes	Yes	Yes	0.55
M8	Yes	Yes	Yes	Yes	Yes	0.55
M9	Yes	Yes	Yes	Yes	Yes	0.55
M10	Yes	Yes	Yes	Yes	Yes	0.55
M11	Yes	Yes	Yes	Yes	Yes	0.55
M12	Yes	Yes	Yes	Yes	Yes	0.55
M13	Yes	Yes	Yes	Yes	Yes	0.55
M14	Yes	Yes	Yes	Yes	Yes	0.55
M15	Yes	Yes	Yes	Yes	Yes	0.55
M16	Yes	Yes	Yes	Yes	Yes	0.55
M17	Yes	Yes	Yes	Yes	Yes	0.55
M18	Yes	Yes	Yes	Yes	Yes	0.55
M19	Yes	Yes	Yes	Yes	Yes	0.55
M20	Yes	Yes	Yes	Yes	Yes	0.55
M21	Yes	Yes	Yes	Yes	Yes	0.55
M22	Yes	Yes	Yes	Yes	Yes	0.55
M23	Yes	Yes	Yes	Yes	Yes	0.55
M24	Yes	Yes	Yes	Yes	Yes	0.55
M25	Yes	Yes	Yes	Yes	Yes	0.55

3.3. ADME result.

The studied molecules were evaluated for their ADME properties to determine their suitability as future drugs. The outcomes are shown in Table 5.

As mentioned in Table 5, all tested molecules have high absorption and are poorly distributed in the brain. For the CNS index, substances with LogPS > -2 are thought to be able to penetrate the CNS, while substances with LogPS <-3 are thought to be unable to do so [47]. Thus, the 25 molecules are unable to enter the central nervous system (Table 5). Moreover, all molecules were found to be no substrate for P-glycoprotein. A substance's potential toxicity and drug interactions must be tested for its ability to inhibit the cytochrome P450 (CYP) enzymes. In fact, substrates of the five major isoforms comprise 50% of all pharmacological substances (CYP1A2, CYP2C19, CYP2C9, CYP2D6, and CYP3A4). The metabolism of drugs is greatly influenced by these enzymes. The result of Table 5 indicates that all the molecules inhibit the isoforms CYP2C9, CYP2D6, and CYP3A4. For the isoforms CYP1A2 andCYP2C19, there are compounds that inhibit them and others that do not. On the other hand, the smaller the clearance value, the more persistent the medication is in the body. The outcomes in Table 5 indicate that the 25 molecules examined can be deemed safe drugs.

Table 5. ADME properties results of the 25 studied derivatives.

Comp.	GI absorption	BBB permeant	CNS permeability Numeric (log PS)	P-gp substrate	CYP1A2 inhibitor	CYP2C19 inhibitor	CYP2C9 inhibitor	CYP2D6 inhibitor	CYP3A4 inhibitor	Clearance
M1	High	No	-2.792	No	No	No	No	No	No	0.28
M2	High	No	-2.545	No	No	No	No	No	No	0.365
M3	High	No	-2.535	No	No	No	No	No	No	0.539
M4	High	Yes	-2.339	No	No	No	No	No	No	0.546
M5	High	Yes	-2.324	No	No	No	No	No	No	0.598
M6	High	No	-2.523	No	No	No	No	No	No	0.564
M7	High	Yes	-2.243	No	Yes	Yes	No	No	No	0.189
M8	High	Yes	-2.556	No	Yes	Yes	No	No	No	0.59
M9	High	Yes	-2.375	No	Yes	Yes	No	No	No	0.64
M10	High	Yes	-2.847	No	Yes	Yes	No	No	No	0.768
M11	High	No	-2.231	No	Yes	Yes	No	No	No	0.284
M12	High	No	-2.424	No	Yes	Yes	No	No	No	0.624
M13	High	No	-2.075	No	Yes	Yes	No	No	No	0.204
M14	High	No	-2.529	No	No	No	No	No	No	0.429
M15	High	No	-2.527	No	Yes	No	No	No	No	0.475
M16	High	No	-2.542	No	Yes	No	No	No	No	0.524
M17	High	Yes	-2.355	No	Yes	No	No	No	No	0.538
M18	High	No	-2.522	No	Yes	No	No	No	No	0.635
M19	High	No	-2.519	No	Yes	No	No	No	No	0.472
M20	High	No	-2.412	No	Yes	Yes	No	No	No	0.130
M21	High	Yes	-2.569	No	Yes	Yes	No	No	No	0.724
M22	High	Yes	-2.847	No	Yes	No	No	No	No	0.669
M23	High	Yes	-2.832	No	Yes	Yes	No	No	No	0.700
M24	High	Yes	-2.457	No	Yes	Yes	No	No	No	0.623
M25	High	Yes	-2.116	No	Yes	Yes	No	No	No	0.068

3.4. Toxicity result.

In this section, the 25 selected compounds were investigated for their toxicity using four toxicological endpoints: mutagenicity, hepatotoxicity, carcinogenicity, and rat acute toxicity LD50 value, and their results are shown in Table 6. The Ames test has been used to assess whether or not a molecule is mutagenic. Except for molecules **M1**, **M12**, **M13**, **M24,** and **M25**, all molecules were found to be no toxic. Moreover, all the molecules studied do not show any hepatotoxicity or carcinogenicity. Regarding Oral Rat Acute Toxicity, a substance with a lower LD50 is more lethal than a substance with a higher LD50. The outcomes in Table 6 reveal that all the molecules studied are safe.

Table 6. Toxicity prediction of the 25 2-methoxy benzoyl hydrazone compounds.

Compound	Ames toxicity test	Hepatotoxicity	Carcinogenicity	Oral Rat Acute Toxicity (LD50: mol/Kg)
M1	Yes-toxic	No-hepatotoxic	Non-carcinogen	1.723
M2	No-toxic	No-hepatotoxic	Non-carcinogen	1.986
M3	No-toxic	No-hepatotoxic	Non-carcinogen	1.831
M4	No-toxic	No-hepatotoxic	Non-carcinogen	1.831
M5	No-toxic	No-hepatotoxic	Non-carcinogen	2.025
M6	No-toxic	No-hepatotoxic	Non-carcinogen	2.014
M7	No-toxic	No-hepatotoxic	Non-carcinogen	2.375
M8	No-toxic	No-hepatotoxic	Non-carcinogen	2.097
M9	No-toxic	No-hepatotoxic	Non-carcinogen	1.954
M10	No-toxic	No-hepatotoxic	Non-carcinogen	2.055

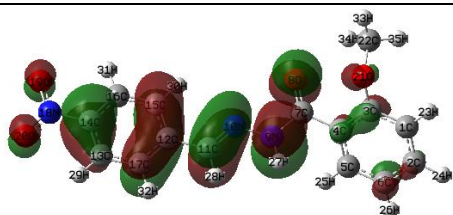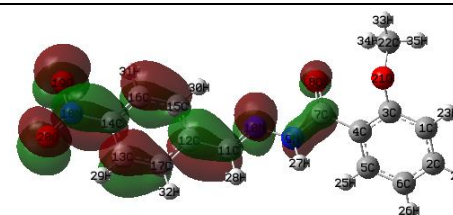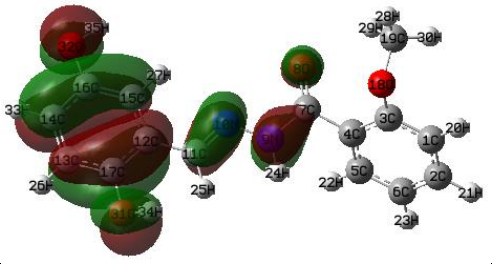| Compound	Ames toxicity test	Hepatotoxicity	Carcinogenicity	Oral Rat Acute Toxicity (LD50: mol/Kg)
M11	No-toxic	No-hepatotoxic	Non-carcinogen	2.153
M12	Yes-toxic	No-hepatotoxic	Non-carcinogen	2.320
M13	Yes-toxic	No-hepatotoxic	Non-carcinogen	2.147
M14	No-toxic	No-hepatotoxic	Non-carcinogen	1.931
M15	No-toxic	No-hepatotoxic	Non-carcinogen	1.802
M16	No-toxic	No-hepatotoxic	Non-carcinogen	1.947
M17	No-toxic	No-hepatotoxic	Non-carcinogen	2.228
M18	No-toxic	No-hepatotoxic	Non-carcinogen	2.084
M19	No-toxic	No-hepatotoxic	Non-carcinogen	2.288
M20	No-toxic	No-hepatotoxic	Non-carcinogen	2.467
M21	No-toxic	No-hepatotoxic	Non-carcinogen	2.046
M22	No-toxic	No-hepatotoxic	Non-carcinogen	2.202
M23	No-toxic	No-hepatotoxic	Non-carcinogen	2.022
M24	Yes-toxic	No-hepatotoxic	Non-carcinogen	1.938
M25	Yes-toxic	No-hepatotoxic	Non-carcinogen	2.238

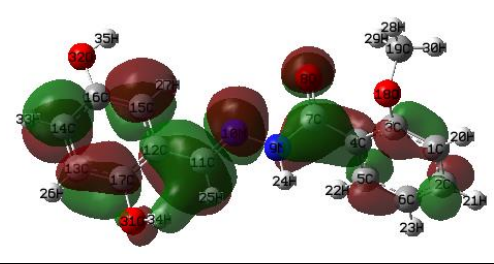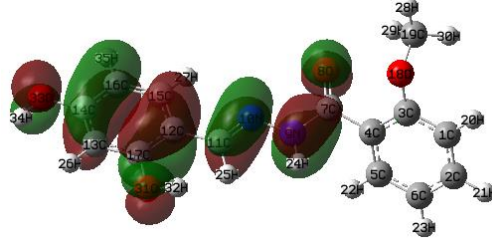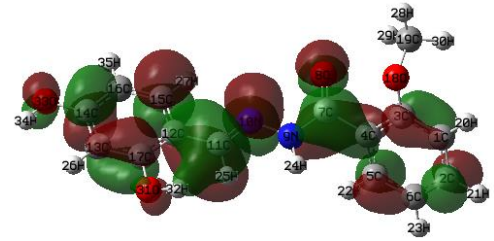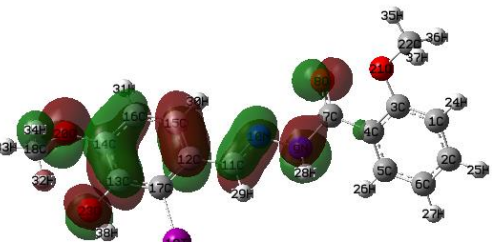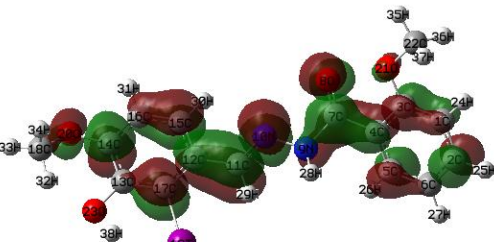*3.5. Global properties of the selected compounds.*

The global reactivity indices of the selected molecules **M12**, **M15**, **M16,** and **M20** were calculated and listed in Table 7. The compounds **M12** and **M20** have an electrophilicity index ω of 3.540 and 3.468, respectively, and nucleophilicity index N value of 2.408 eV and 2.638, respectively. These compounds have been classified as powerful electrophiles based on the electrophilicity scale [48]. Compounds **M15** and **M16** have a nucleophilicity N value of 3.506 and 3.532 eV, respectively, and an electrophilicity ω value of 1.863 and 1.649, respectively. Thus, based on the nucleophilicity scale, these molecules are considered strong nucleophiles [49]. Additionally, the Frontier Molecular Orbitals (FMOs) of the selected molecules were studied at the B3LYP/6–311++G (d,p) level of theory, and their graphs are listed in Table 8. The HOMO-LUMO energy gap was calculated for each molecule; in fact, a high value of ΔEgap implies low chemical reactivity as it is energetically disfavored to add an electron to the high-level LUMO to extract electrons from the low-level HOMO [50,51]. The obtained values of ΔE_{gap} revealed the high chemical reactivity of the selected molecules.

Table 7. Global properties of the selected compounds.

Compound	Global properties						
	HOMO (ev)	LUMO (ev)	μ (ev)	η (ev)	S (ev)	ω (ev)	N (ev)
M12	-6.960	-3.267	-5.113	3.693	0.270	**3.540**	2.408
M15	-5.862	-1.861	-3.861	4.001	0.249	1.863	**3.506**
M16	-5.836	-1.622	-3.72	4.214	0.237	1.649	**3.532**
M20	-6.73	-3.186	-4.958	3.544	0.282	**3.468**	2.638

Table 8. The HOMO and LUMO orbital forms, as well as the energy gap value, computed at the B3LYP/6–311++G (d,p) calculation level of the selected inhibitors.
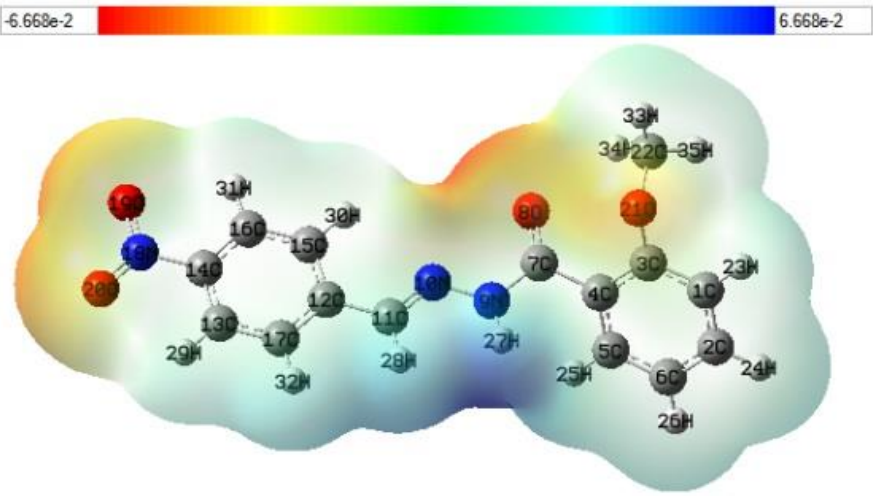
| Comp	HOMO orbital	LUMO orbital	ΔEgap
M12			3.693

Comp	HOMO orbital	LUMO orbital	ΔEgap
M15			4.001
M16			4.214
M20			3.544

3.6. Molecular electrostatic potential (MEP).

Molecular electrostatic potential (MEP) maps have been performed to discover the regions of electrophilic and nucleophilic reactivity of an organic compound. The MEP surfaces of the studied molecules were constructed using the B3LYP/6-311++G (d,p) level available in the Gaussian program. The MEP maps of the molecules **M12**, **M15**, and **M16** are displayed in Table 9. The positive (electron-poor) portion is shown in blue, the slightly electron-deficient region is shown in light blue, the neutral region is shown in green, the negative (electron-rich) part is shown in red, and the somewhat electron-rich part is shown in yellow.

Table 9. The electrostatic potential surface of the selected molecules**.**

Comp	Electrostatic potential surface
M12	

Comp	Electrostatic potential surface
M15	
M16	
M20	
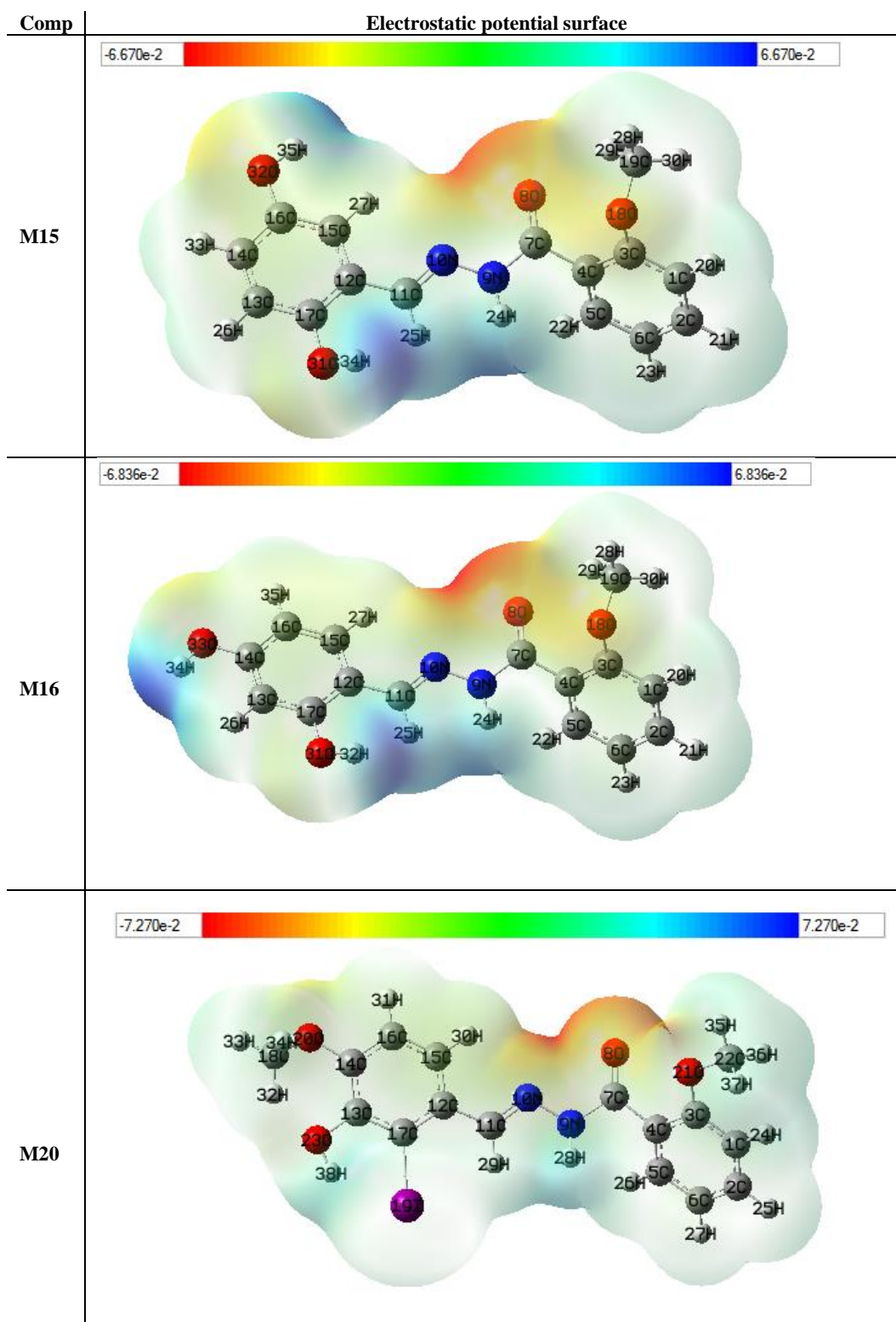
The molecule **M12** shows a faint negative potential (yellowish color) at the level of 19O, 20O, and 18N of the nitrogen oxide group and 8O, 21O of the ketone and methoxy groups, respectively. While the molecule **M12** shows a low positive potential (light blue) at the level of all carbon atoms of the concerned molecule. Thus, we can conclude that 19O, 20O, 18N, 8O, and 21O are the favorite sites for electrophilic attack. Moreover, In the case of compounds **M15**, **M16,** and **M18,** the 8O and 21O of the ketone and methoxy groups, respectively, which represent the low electron density potions, are the preferred sites for the electrophilic attack.

4. Conclusions

A molecular modeling study on a series of twenty-five 2methoxy benzoyl hydrazone derivatives as antileishmanial inhibitors has been executed using molecular docking and ADMET analysis. The results show that all molecules are stable in the active pocket of the receptor. Compounds **M12**, **M15**, **M16,** and **M20** reveal a good binding energy value and exhibit many types and numbers of interactions. These compounds showed good absorption, distribution, and metabolism and were found to be non-toxic with the exception of compound **M20**. Furthermore, the quantum study using the DFT approach identified compounds **M15** and **M16** as strong nucleophiles while compound **M12** was a strong electrophile. Therefore, the selected molecules could be used as antileishmanial drug candidates.

Funding

Acknowledgments

Conflicts of Interest

The authors declare no conflict of interest in the study.

References

1. Maciel, M.S.P.; Reis, A.S.D.; Fidelis, Q.C. Antileishmanial potential of species from the family Lamiaceae: chemical and biological aspects of non-volatile compounds. *Acta Trop* **2022**, *228*, 106309, https://doi.org/10.1016/j.actatropica.2022.106309.
2. World Health Organization (WHO). Leishmaniasis **2021**. https://www.who.int/news-room/fact-sheets/detail/leishmaniasis (accessed on 20 June, 2022).
3. Ribeiro, J.M.; Rodrigues-Alves, M.L.; Oliveira, E.; Guimarães, P.P.G.; Murta Santi, A.M.; Teixeira-Carvalho, A.; Murta, S.M.F.; Peruhype-Magalhães, V.; Souza-Fagundes, E.M. Pamidronate, a promising repositioning drug to treat leishmaniasis, displays antileishmanial and immunomodulatory potential. *Int Immunopharmacol* **2022**, *110*, 108952, https://doi.org/10.1016/j.intimp.2022.108952.
4. Burza, B.; Croft, S.L.; Boelaert, M. Leishmaniasis. *The Lancet* **2018**, 951-970, https://doi.org/10.1016/S0140-6736(18)31204-2.
5. Guerin, P.J.; Olliaro, P.; Sundar, S.; Boelart, M.; Croft, S.L.; Desjeux, P.; Wasunna, M.K.; Bryceson, A.D.M. Visceral leishmaniasis: current status of control, diagnosis, and treatment, and a proposed research and development agenda. *The Lancet Infectious Diseases* **2002**, 494-501, https://doi.org/10.1016/s1473-3099(02)00347-x.
6. Croft, S.L. Recent developments in the chemotherapy of leishmaniasis. *Trends Pharmacol Sci* **1988**, *9*, 376-381, https://doi.org/10.1016/0165-6147(88)90258-1.
7. Berman, J.D. Chemotherapy for leishmaniasis: biochemical mechanisms, clinical efficacy, and future strategies. *Rev Infect Dis* **1988**, *10*, 560-586, https://doi.org/10.1093/clinids/10.3.560.
8. Murray, H.W. Treatment of visceral leishmaniasis in 2004. *Am J Trop Med Hyg* **2004**, *71*, 787-794.
9. Santos, S.S.; Araújo, R.V.; Giarolla, J.; Seoud, O.E.; Ferreira, E.I. Searching for drugs for Chagas disease, leishmaniasis and schistosomiasis: a review. *Int J Antimicrob Agents* **2020**, *55*, 105906, https://doi.org/10.1016/j.ijantimicag.2020.105906.
10. Panneerselvam, P.; Rather, B. A.; Reddy, D. R. S.; Kumar, R. N. Synthesis and antimicrobial screening of some Schiff bases of 3-amino-6,8-dibromo-2-phenylquinazolin-4(3H)-ones. *Eur J Med Chem* **2009**, *44*, 2328, https://doi.org/10.1016/j.ejmech.2008.04.010.

11. Pandeya, S. N.; Sriram, D.; Nath, G.; DeClercq, E. Synthesis, antibacterial, antifungal and anti-HIV activities of Schiff and Mannich bases derived from isatin derivatives and N-[4-(4'-chlorophenyl)thiazol-2-yl] thiosemicarbazide. *Eur J Pharm Sci* **1999**, *9*, 25-31, https://doi.org/10.1016/s0928-0987(99)00038-x.

12. Karthikeyan, M. S.; Prassad, D. J.; Poojary, B.; Bhat, K. S.; Holla, B. B.; Kumari, N.S. Synthesis and biological activity of Schiff and Mannich bases bearing 2,4-dichloro-5-fluorophenyl moiety. *Bioorg Med Chem* **2006**, *14*, 7482-7489, https://doi.org/10.1016/j.bmc.2006.07.015.

13. Pervaiz, M.; Munir, A.; Riaz, A.; Saeed, Z.; Younas, U.; Imran, M.; Ullah, S.; Bashir, R.; Rashid, A.; Adnan, A. Review article-Amalgamation, scrutinizing, and biological evaluation of the antimicrobial aptitude of thiosemicarbazide Schiff bases derivatives metal complexes. *Inorg Chem Comms* **2022**, *141*, 109459, https://doi.org/10.1016/j.inoche.2022.109459.

14. Gupta, D.; Pathak, D.P.; G. Kapoor, G.; R. Bhutani, R.; A comprehensive review on synthesis and biological activity of Schiff bases. Int Res J Pharm **2019**, *10*, 1–8, https://doi.org/10.7897/2230-8407.1005153.

15. Karem, L.K.A.; Waddai, F.Y.; Karam, N.H. Schiff base complexes of some drug substances (Review). *J Pharm Sci Res* **2018**, *10*, 1912–1917.

16. Toubi, Y.; Abrigach, F.; Radi, S.; Souna, F.; Hakkou, A.; Alsayari, A.; Bin Muhsinah, A.; Mabkhot, Y.N. Synthesis, antimicrobial screening, homology modeling, and molecular docking studies of a new series of Schiff base derivatives as prospective fungal inhibitor candidates. *Molecules* **2019**, *24*, 3250–3265, https://doi.org/10.3390/molecules24183250.

17. Khaldan, A.; Bouamrane, S.; El-Mernissi, R.; Maghat, H.; Ajana, A.; Sbai, A.; Bouachrine, M.; Lakhlifi, T. Identification of Potential α-Glucosidase Inhibitors: 3D-QSAR Modeling, Molecular Docking Approach. *Rhazes: Green and applied chemistry* **2021**, *12*, 60-75.

18. El Khatabi, K.; Aanouz, I.; El-Mernissi, R.; Khaldan, A.; Ajana, M.; Bouachrine, M.; Lakhlifi, T. In Silico Analysis of 3D QSAR and Molecular Docking Studies to Discover New Thiadiazole-Thiazolone Derivatives as Mitotic Kinesin Eg5 Inhibition. Moroc. J. Chem. **2021**, *9*, 9–405, https://doi.org/10.48317/IMIST.PRSM/morjchem-v9i2.18721.

19. Khaldan, A.; Bouamrane, S.; El-Mernissi, R.; El Khatabi, K.; Aanouz, I.; Aggoram, A.; Sbai, A.; Bouachrine, M.; Lakhlifi, T. QSAR Study of α-Glucosidase Inhibitors for Benzimidazole Bearing Bis-Schiff Bases Using CoMFA, CoMSIA, and Molecular Docking. *Int J Quant. Struct.-Prop Relatio* **2021**, *6*, 9–24, https://doi.org/10.4018/IJQSPR.2021010102.

20. Khaldan, A.; El khatabi, K.; El-Mernissi, R.; Ghaleb, A.; Hmamouchi, R.; A.; Sbai, A.; Bouachrine, M.; Lakhlifi, T. 3D-QSAR Modeling and Molecular Docking Studies of novel triazoles-quinine derivatives as antimalarial agents. *J Mater Environ Sci* **2020**, *11*, 429-443.

21. Khaldan, A.; Bouamrane, S.; El-mernissi, R.; Ajana, M.A.; Sbai, A.; Bouachrine, M.; Lakhlifi, T. In silico design of new α-glucosidase inhibitors through 3D-QSAR study, molecular docking modeling and ADMET analysis. *Mor J Chem* **2022**, *10*, 022-036, https://doi.org/10.48317/IMIST.PRSM/MORJCHEM-V10I1.31722.

22. Khaldan, A.; Bouamrane, S.; El-mernissi, R.; Maghat, H.; Ajana, M.A.; Sbai, A.; Bouachrine, M.; Lakhlifi, T. 3D-QSAR modeling, molecular docking and ADMET properties of benzothiazole derivatives as α-glucosidase inhibitors. *Materials Today: Proceedings* **2021**, *45*, 7643–7652, https://doi.org/10.1016/j.matpr.2021.03.114.

23. Khaldan, A.; Bouamrane, S.; En-Nahli, F.; El-mernissi, El khatabi, R.; El khatabi, K.; Hmamouchi, R.; Maghat, H.; Ajana, M.A.; Sbai, A.; Bouachrine, M.; Lakhlifi, T. Prediction of potential inhibitors of SARS-CoV-2 using 3D-QSAR, molecular docking modeling and ADMET properties. *Heliyon* **2021**, *7*, e06603, https://doi.org/10.1016/j.heliyon.2021.e06603.

24. Khaldan, A.; Bouamrane, S.; El-mernissi, R.; Maghat, H.; Ajana, M.A.; Sbai, A.; Bouachrine, M.; Lakhlifi, T. In silico study of 2,4,5-trisubstituted thiazoles as inhibitors of tuberculosis using 3D-QSAR, molecular docking, and ADMET analysis. *El-Cezerî Journal of Science and Engineering* **2022**, *9*, 452-468, https://doi.org/10.31202/ecjse.961940.

25. El-Mernissi, R.; El Khatabi, K.; Khaldan, A.; ElMchichi, L.; Shahinozzaman, M.; Ajana, M.A.; Lakhlifi, T.; Bouachrine, M. 2-Oxoquinoline Arylaminothiazole Derivatives in Identifying Novel Potential Anticancer Agents by Applying 3D-QSAR, Docking, and Molecular Dynamics Simulation Studies. *J. Mex Chem Soc* **2021**, *66*, 79-94, https://doi.org/10.29356/jmcs.v66i1.1578.

26. Bouamrane, S.; Khaldan, A.; H. Hajji, H.; El-mernissi, R.; Maghat, H.; Ajana, M.A.; Sbai, A.; Bouachrine, M.; Lakhlifi, T. 3D-QSAR, molecular docking, molecular dynamic simulation, and ADMET study of

bioactive compounds against candida albicans. *Mor J Chem* **2022**, *10*, 523-541, https://doi.org/10.48317/IMIST.PRSM/morjchem-v10i3.33141.

27. El-Mernissi, R.; El Khatabi, K.; Khaldan, A.; El Mchichi, L.; Ajana, M.A.; Lakhlifi, T.; Bouachrine, M. Design of new 3, 5-disubstituted indole as hematological anticancer agents using 3D-QSAR, molecular docking and drug-likeness studies. *Materials Today: Proceedings* **2021**, *45*, 7608-7614, https://doi.org/10.1016/j.matpr.2021.03.080.

28. Taha, M.; Baharudin M.S.; Ismail N.H.; Khan K.M.; Jaafar F.M.; Samreen; Siddiqui S.; Choudhary, M.I. Synthesis of 2-methoxybenzoylhydrazone and evaluation of their antileishmanial activity. *Bioorg Med Chem Lett* **2013**, *23*, 3463-6, https://doi.org/10.1016/j.bmcl.2013.03.051.

29. Frisch, M. GAUSSIAN 09, **2009** (2009) Revision E. 01, Gaussian Inc.

30. Nawaz, M.Z.; Attique, S.A.; Ain, Q.U.; Alghamdi, H.A.; Bilal, M.; Yan, W.; Zhu, D. Discovery and characterization of dual inhibitors of human Vanin-1 and Vanin-2 enzymes through molecular docking and dynamic simulation-based approach. *Int J Biol Macromol* **2022**, *213*, 1088-1097, https://doi.org/10.1016/j.ijbiomac.2022.06.014.

31. Trott, O.; Olson, A.J. AutoDock Vina: Improving the speed and accuracy of docking with a new scoring function, efficient optimization, and multithreading. *J Comput Chem* **2009**, NA-NA, https://doi.org/10.1002/jcc.21334.

32. Hunter, C.A.; Lawson, K.R.; Perkins, J.; Urch, C.J. Aromatic interactions. *J Chem Soc, Perkin Trans 2* **2001**, 651–669, https://doi.org/10.1039/b008495f.

33. Baiocco, P.; Colotti, G.; Franceschini, S.; Ilari, J. Molecular basis of antimony treatment in leishmaniasis. *J Med Chem* **2009**, *52*, 2603-2612, https://doi.org/10.1021/jm900185q.

34. Aziz, H.; Saeed, A.; Jabeen, F.; Simpson, J.; Munawar, A.; Qasim, M. Synthesis, crystal structure, cytotoxic, antileishmanial activities and docking studies on N,N0-(ethane-1,2-diyl)bis(3-methylbenzamide). *J Mol Struct* **2008**, *1156*, 627-631, https://doi.org/10.1016/j.molstruc.2017.12.010.

35. Dassault Syst`emes BIOVIA Discovery Studio Modeling Environment Release 2017 Dassault Syst`emes, **2016**.

36. Belhassan, A.; Zaki, H.; Chtita, S.; Alaqarbeh, M.; Alsakhen, N.; Benlyas, M.; Lakhlifi, T.; Bouachrine, M. Camphor, Artemisinin and Sumac Phytochemicals as inhibitors against COVID-19: Computational approach. *Comput Biol Med* **2021**, *136*, 104758, https://doi.org/10.1016/j.compbiomed.2021.104758.

37. Pires, D.E.V.; Blundell, T.L.; Ascher, D.B. pkCSM: Predicting Small-Molecule Pharmacokinetic and Toxicity Properties Using Graph-Based Signatures. *J Med Chem* **2015**, *58*, 4066–4072, https://doi.org/10.1021/acs.jmedchem.5b00104.

38. Daina, A.; Michielin, O.; Zoete, V. SwissADME: a free web tool to evaluate pharmacokinetics, drug-likeness and medicinal chemistry friendliness of small molecules. *Sci Rep* **2017**, *7*, 42717, https://doi.org/10.1038/srep42717.

39. Pearson, R.G.; Songstad, J. Application of the Principle of Hard and Soft Acids and Bases to Organic Chemistry. *J Am Chem Soc* **1967**, *89*, 1827–1836, https://doi.org/10.1021/ja00984a014.

40. Parr, R.G.; von Szentpály, L.; Liu, S. Electrophilicity Index. *J Am Chem Soc* **1999**, *121*, 1922–1924, https://doi.org/10.1021/ja983494x.

41. Domingo, L.R.; Chamorro, E.; Pérez, P. Understanding the Reactivity of Captodative Ethylenes in Polar Cycloaddition Reactions. A Theoretical Study. *J Org Chem* **2008**, *73*, 4615–4624, https://doi.org/10.1021/jo800572a.

42. Domingo, L.R.; Pérez, P. The nucleophilicity N index in organic chemistry. *Org Biomol Chem* **2011**, *9*, 7168-7175, https://doi.org/10.1039/c1ob05856h.

43. Ortiz, C.L.D.; Completo, G.C.; Nacario, R.C.; Nellas, R.B. Potential Inhibitors of Galactofuranosyltransferase 2 (GlfT2): Molecular Docking, 3D-QSAR, and In Silico ADMETox Studies. *Sci Rep* **2019**, *9*, 17096, https://doi.org/10.1038/s41598-019-52764-8.

44. Kramer, B.; Rarey, M.; Lengauer, T. Evaluation of the FLEXX incremental construction algorithm for protein-ligand docking. *Proteins* **1999**, *37*, 228–241, https://doi.org/10.1002/(sici)1097-0134(19991101)37:2<228::aid-prot8>3.0.co;2-8.

45. Teague, S.J.; Davis, A.M.; Leeson, P.D.; Oprea, T. The Design of Leadlike Combinatorial Libraries. *Angew Chem Int Ed Engl* **1999**, *38*, 3743-3748, https://doi.org/10.1002/(SICI)1521-3773(19991216)38:24<3743::AID-ANIE3743>3.0.CO;2-U.

46. Martin, Y.C. A bioavailability score. *J Med Chem* **2005**, *48*, 3164–3170, https://doi.org/10.1021/jm0492002.

47. Han, Y.; Zhang, J.; Hu, C.Q.; Zhang, X.; Ma, B. Zhang, P. In silico ADME and toxicity prediction of ceftazidime and its impurities. *Front Pharmacol* **2019**, *10*, https://doi.org/10.3389/fphar.2019.00434.

48. Jaramillo, P.; Domingo, L.R.; Chamorro, E.; Pérez, P. A further exploration of a nucleophilicity index based on the gas-phase ionization potentials. J Mol Struct: THEOCHEM **2008**, *865*, 68–72, https://doi.org/10.1016/j.theochem.2008.06.022.

49. Domingo, L.R.; Aurell, M.J.; Pérez, P.; Contreras, R. Quantitative characterization of the global electrophilicity power of common diene/dienophile pairs in Diels–Alder reactions. Tetrahedron **2002**, *58*, 4417–4423, https://doi.org/10.1016/S0040-4020(02)00410-6.

50. Manolopoulos, D.E.; May, J.C.; Down, S.E. Theoretical studies of the fullerenes: C34 to C70. Chem Phys Lett **1991**, *181*, 105-111, https://doi.org/10.1016/0009-2614(91)90340-F.

51. Ruiz-Morales, Y. HOMO−LUMO Gap as an Index of Molecular Size and Structure for Polycyclic Aromatic Hydrocarbons (PAHs) and Asphaltenes: A Theoretical Study. I, J Phys Chem A **2002**, *106*, 11283-11303, https://doi.org/10.1021/jp021152e.